Bulletin of the Czech Geological Survey, Vol. 77, No. 4, 243–252, 2002

Asteroids: Their composition and impact threat

THOMAS H. BURBINE

Department of Mineral Sciences, National Museum of Natural History, Smithsonian Institution, Washington, DC 20560-0119, USA; e-mail: burbine.tom@nmnh.si.edu

Abstract. Impacts by near-Earth asteroids are serious threats to life as we know it. The energy of the impact will be a function of the mass of the asteroid and its impact velocity. The mass of an asteroid is very difficult to determine from Earth. One way to derive a near-Earth object's mass is by estimating the object's density from its surface composition. Reflectance spectra are the best way to determine an object's composition since many minerals (e.g. olivine, pyroxene, hydrated silicates) have characteristic absorption features. However, metallic iron does not have characteristic absorption bands and is very hard to identify from Earth. For a particular size, asteroids with compositions similar to iron meteorites pose the biggest impact threat since they have the highest densities, but they are expected to be only a few percent of the impacting population. Knowing an asteroid's composition is also vital for understanding how best to divert an incoming asteroid.

Key words: Earth, asteroids, impact features, meteorites, mineral composition, geologic hazards

Introduction

As we enter a new millennium, we are constantly being bombarded with news of close encounters with near-Earth objects (NEOs). Observers have discovered over 2,000 near-Earth asteroids (NEAs); luckily none are known to be on a collision course with the Earth. Comets are also serious impact threats as shown by the collision of Shoemaker-Levy-9 with Jupiter in 1994. Since the discovery of the iridium anomaly at the Cretaceous-Tertiary (K-T) boundary layer by Alvarez et al. (1980), there has been a considerable discussion of the possibility and consequences of such an impact (e.g. Chapman and Morrison 1994, Adushkin and Nemchinov 1994, Toon et al. 1997, Garshnek et al. 2000).

As we discover more Earth-approaching asteroids, we are also learning more about their compositions and structure. Charge-coupled devices (CCDs) now allow us to obtain visible and near-infrared telescopic spectra of near-Earth asteroids that are a few hundred meters or smaller in diameter (e.g. Binzel et al. 2001a). Technological improvements to the radio telescope at the Arecibo Observatory have allowed similarly sized objects to be characterized by radar (e.g. Ostro et al. 2002). Spacecraft missions now show asteroids to be geologic bodies with a variety of morphologic features. More meteorites are discovered every year and are being extensively studied in the laboratory with more precise analytical techniques.

However as we continue our research on asteroids, a number of questions should be asked. "How do asteroid compositions affect the impact threat?" "How well can we determine asteroid compositions from Earth?" This paper will review what we currently know about asteroid compositions and how it affects the impact threat. Since we have not yet returned any samples from any asteroids, our knowledge of asteroid compositions is derived from analyses of meteorites, remote sensing observations from Earth, and spacecraft missions.

Impact threat

I will first briefly review what we know about the number of near-Earth objects and the energy and effects of impacts. The near-Earth object population is defined as small bodies with perihelion distance less than 1.3 AU (astronomical units) and aphelion distance greater than 0.983 AU (Morbidelli et al. 2002). These objects are primarily thought to be asteroids ejected from the main belt; however, a few extinct comets probably exist in the population. Recent estimates of the numbers of NEAs larger than one kilometer in diameter vary from 855 (±110) (Morbidelli et al. 2002) to 1227 (uncertainties of +170 and –90) (Stuart 2001).

The kinetic energy (E) of an incoming asteroid is $(1/2)mv^2$ where m is the mass and v is the velocity. Mass is a function of the density (ρ) and volume (V) of the object. Since the energy of an impact is usually given as megatons of TNT, the kinetic energy equation can be written (Morbidelli et al. 2002) as

$$E = 62.5\ \rho d^3 v^2$$

where E is in megatons, ρ is in g/cm^3, d is the diameter of the impactor in kilometers, and v is in km/s. The average impact velocity for asteroids with Earth are ~ 20 km/s (e.g. Hughes, 1998). Comets have lower densities (estimated to be around ~ 1 g/cm^3), but some long-period comets have much higher average impact velocities (~ 55 km/s) (Marsden and Steel 1994). Since water covers approximately three-fourths of the Earth's surface, "large" impacts are likely to cause tsunamis (e.g. Paine 1999), giant tidal waves created by sudden disturbances.

The best-characterized localized catastrophe is the impact at Tunguska where an object exploded 5–10 km in the air over an uninhabited region of Siberia (e.g. Chyba et al. 1993, Vasilyev 1998). The energy was estimated to be ~ 10–20 megatons and devastated an area of ~ 2000 km^2 of forest area. In comparison, the energy is ~ 1,000 times larger than the bomb dropped on Hiroshima and the area is ~ 4 times larger than New York City.

The best-characterized "large" impact is the Chicxulub crater found in the Yucatan peninsula (e.g. Hildebrand et al. 1998). Hildebrand et al. (1998) argues that the crater is 180 km in diameter, but other researchers (e.g. Morgan et al. 1998) argue that the actual crater size could be as large as 270 km. The energy of the impactor for producing the Chicxulub crater is estimated to be ~ 10^8 megatons (e.g. Toon et al. 1997). This impact occurred ~ 65 million years ago, which is the same age as the K-T extinction. The K-T boundary marks the demise of the dinosaurs as the dominant animal species on Earth (e.g. Milner 1998).

We currently have evidence for over 160 impact craters on Earth over the last ~ 2 billion years that range from 15 meters to 300 kilometers in diameter (Earth Impact Database 2002). Many more impacts have occurred over this time with evidence for these impacts wiped out due to erosion by water and wind. Cratering rates for the Earth (e.g. Neukum and Ivanov, 1994) can be estimated from determinations of the NEO population, the lunar cratering rate (where the effects of the Earth's atmosphere needed to be added), and crater counts on terrestrial cratons. Neukum and Ivanov (1994) estimate that craters one kilometer in size or greater form on the Earth every ~ 1600 years and craters 100 kilometers in size or greater form every 27 million years.

Morbidelli et al. (2002) have done a recent study of collision probabilities of NEOs with the Earth. They estimate that a 1000 megaton impact, which would produce large-scale regional damage and a crater ~ 5 km in size (e.g. Hughes 1998), should occur every 63,000 ± 8,000 years. They estimate that known NEOs carry only ~ 18% of the overall collision probability.

The consequences of any impact on Earth will be a function of the mass (density times volume) and impact velocity plus the location, date, and time of the impact on Earth. Astrometric observations, which determine the location of an object in the sky, can help determine an asteroid's orbit with a high degree of certainty. These observations can be used to predict the probability that an object will strike the Earth. If an object is on a collision course these astrometric observations can be used to predict the impact velocity and the location of the impact. Radar observations (e.g. Ostro et al. 2002) can image an asteroid (if it is large enough and close enough to Earth) and then determine its diameter, which can be used to calculate its volume.

However, the determination of an asteroid's mass is much more difficult from Earth. For the largest asteroids, masses can be determined by asteroid-asteroid interactions or their perturbations on Mars (Britt et al. 2002). To determine a near-Earth asteroid's mass, the object needs to have a natural body revolving around it (e.g. Margot et al. 2002) or a spacecraft encounter (e.g. Veverka et al. 1999, Yeomans et al. 2000).

However in the absence of such a mass determination, the best way to estimate a near-Earth asteroid's mass would be to determine its surface composition, which would give insight into the object's density. (Since near-Earth asteroids are fragments of much larger asteroids, we assume that the surface composition is representative of the object as a whole.) The mass could then be estimated by multiplying the inferred density by the object's volume. Such an estimate would only give an upper limit on an object's mass, since many asteroids are thought to be rubble piles with significant amounts of macroporosity (e.g. Britt and Consolmagno 2001, Britt et al. 2002). The estimated macroporosities for ~ 20 asteroids range from 0 to ~ 80% (Britt et al. 2002).

Meteorites

Except for ~ 50 samples from the Moon and Mars, meteorites appear to be fragments of sub-planetary sized bodies (asteroids) that formed ~ 4.56 billion years ago. Meteorites can basically be broken into two types: those that experienced heating but not melting (chondrites) (e.g. Brearley and Jones 1998) and those that experienced melting and differentiation (achondrites, stony-irons, irons) (e.g. Mittlefehldt et al. 1998). Silicate-rich meteorites are often referred to as stony and would include all chondrites and achondrites. Meteorites that are similar in terms of petrologic, mineralogical, bulk chemical, and isotopic properties are separated into groups (Table 1). In general, groups contain five or more members to allow for the compositional characteristics of the group to be adequately characterized.

Currently, 13 groups (Table 1) of chondritic meteorites have been defined. Chondritic groups are subdivided according to petrologic type (1–6) with 1 being the most aqueously altered, 3.0 being the least altered, and 6 being heated to the highest temperatures. Mineralogically, meteorites of petrologic type 1 and 2 (CI, CM, CR) have compositions dominated by phyllosilicates. Visually, these meteorites are extremely dark. The other types of carbonaceous chondrites (CH, CV, CO, CK) tend to have mineralogies dominated by mafic silicates. The R chondrites are dominated by olivine. Ordinary chondrites (H, L, LL) are mixtures of mafic silicates and metallic iron, while enstatite chondrites are composed of enstatite (virtually FeO-free pyroxene) and metallic iron. In addition to these 13 well-defined groups, ~ 14 chondritic grouplets or unique meteorites (Meibom and Clark 1999, Weisberg et al. 2001, Mittlefehldt, 2002) have been recognized.

The differentiated meteorites range from those that experienced only limited differentiation (primitive achondrites) to those (differentiated achondrites, stony-irons, irons) that were produced by extensive melting, melt migration, and fractional crystallization. These processes produce a wide variety of lithologies.

Many of the differentiated meteorites are thought to sample the crusts (howardites, eucrites, and diogenites or HEDs; angrites), core-mantle boundaries (pallasites), and cores (irons) of differentiated bodies. Eucrites contain primarily plagioclase and both low-Ca and high-Ca pyroxenes, while diogenites are predominantly magnesian orthopyroxene. Howardites are breccias of eucritic and diogenitic material. Pallasites are mixtures of metallic iron and olivine. We do not appear to be sampling the mantles of these differentiated bodies (e.g. Burbine et al. 1996); however, we do appear to be sampling the mantles of very-reduced differentiated bodies in the form of aubrites.

Iron meteorites are composed of metallic iron with 5–20% Ni plus accessory phases such as sulfides, schreibersite, and silicate inclusions. Iron meteorites are classified according to siderophile ("iron-loving") element (Ga, Ge, Ir, Ni) concentrations. Of the thirteen groups of iron meteorites, ten (IC, IIAB, IIC, IID, IIF, IIIAB, IIIE, IIIF, IVA, IVB) have fractional crystallization trends suggestive of prolonged cooling as expected from the cores of differentiated bodies. Three of the groups (IAB, IIE, and IIICD) do not display well-developed fractional crystallization trends and contain abundant silicate inclusions, which argues that they are not core fragments. Approximately 90 irons (Grady 2000) are not classified as members of the 13 groups and are labeled anomalous. These ungrouped irons are believed to require 50-70 distinct parent bodies (Wasson 1995, Burbine et al. 2002b).

Other types of differentiated meteorites have undergone varying amounts of melting. These include a number of primitive achondritic meteorites (acapulcoite-lodranites, winonaites), which are samples of partially differentiated asteroids. These meteorites are mixtures of olivine, pyroxene, and metallic iron. Mesosiderites are breccias composed of HED-like clasts of basaltic material mixed with metallic clasts. One possible scenario for the formation of the mesosiderites is the disruption of an asteroid with a molten core (Scott et al. 2001). Rounding out the differentiated meteorites are the olivine-dominated brachinites and the carbon-rich ureilites, whose origins are still being debated (e.g. Mittlefehldt et al. 1998).

Table 1. Meteorite groups

Groups	Composition*	Fall percentages[#] (%)
Carbonaceous chondrites		
CI	phy, mag	0.5
CM	phy, toch, ol,	1.7
CR	phy, px, ol, met	0.3
CO	ol, px, CAIs, met	0.5
CH	px, met, ol,	Only finds
CV	ol, px, CAIs	0.6
CK	ol, CAIs	0.3
Enstatite chondrites		
EH	enst, met, sul, plag, ± ol	0.8
EL	enst, met, sul, plag	0.7
Ordinary chondrites		
H	ol, px, met, plag, sul	34.1
L	ol, px, plag, met, sul	38.0
LL	ol, px, plag, met, sul	7.9
R chondrites	ol, px, plag, sul	0.1
Primitive achondrites		
Acapulcoites[a]	px, ol, plag, met, sul	0.1
Lodranites[a]	px, ol, met, ± plag, ± sul	0.1
Winonaites	ol, px, plag, met	0.1
Differentiated achondrites		
Angrites	TiO_2-rich aug, ol, plag	0.1
Aubrites	enst, sul	0.1
Brachinites	ol, cpx, ± plag	Only finds
Diogenites[b]	opx	1.2
Eucrites[b]	pig, plag	2.7
Howardites[b]	eucritic-diogenitic breccia	2.1
Ureilites	ol, px, graph	0.5
Stony-irons		
Mesosiderites	basalt-met breccia	0.7
Pallasites	ol, met ol, met	0.5
Irons[c]	met, sul, schreib	4.2

Table is revised from tables found in Burbine et al. (2002b).
* Minerals or components are listed in decreasing order of average abundance. Abbreviations: ol – olivine, px – pyroxene, opx – orthopyroxene, pig – pigeonite, enst –enstatite, aug – augite, cpx – clinopyroxene, plag – plagioclase, mag – magnetite, met – metallic iron, sul – sulfides, phy – phyllosilicates, toch – tochilinite, graph – graphite, CAIs – Ca-Al-rich refractory inclusions, schreib – schreibersite, ± – may be present
[#] Fall percentages are calculated from the 942 classified falls that are listed in Grady (2000), Grossman (2000), and Grossman and Zipfel (2001).
[a] Acapulcoites and lodranites appear to come from the same parent body (e.g. Mittlefehldt et al. 1998).
[b] Howardites, eucrites, and diogenites (HEDs) appear to come from the same parent body (e.g. Mittlefehldt et al. 1998).
[c] There are 13 iron meteorite groups plus ~100 ungrouped irons.

Meteorite densities and strengths

Consolmagno and Britt (1998), Flynn et al. (1999), and Wilkinson and Robinson (2000) have recently done studies of meteorite bulk densities. The only CI chondrite measured had a bulk density of 1.58 g/cm^3 while the bulk densities of CM chondrites were 2.08–2.37 g/cm^3. CO chondrites (2.36–2.98 g/cm^3) and CV chondrites (2.60–3.18 g/cm^3) tended to have slightly higher bulk densities. The only enstatite chondrite measured had a bulk density of 3.36 g/cm^3. On average, ordinary chondrites (3.05–3.75 g/cm^3 for the most reliable measurements) have the highest bulk densities of the chondrites.

HEDs have bulk densities of 2.99–3.29 g/cm^3. Stony-irons such as mesosiderites (4.16–4.22 g/cm^3) and pallasites (4.82–4.97 g/cm^3) have higher bulk densities due to the presence of significant amounts of metallic iron. As expected, iron meteorites tend to have the highest bulk densities of all meteorite types (6.99–7.59 g/cm^3 for relatively unweathered specimens).

In terms of physical strength, most chondritic meteorites can be easily crushed into powders with a mortar and pestle. Meteorites containing phyllosilicates tend to be the most fragile with the CI chondrites being the weakest of these objects with laboratory crushing strengths of 1–10 bars (e.g. Lewis 2000). What cannot be easily pulverized is metallic iron. Metallic iron is ductile and tends to flatten and elongate while being crushed at room temperatures. It is unclear how ductile metallic iron is at the colder temperatures found in the asteroid belt.

Iron meteorites are extremely strong with strengths of approximately 3.5 kbars (e.g. Lewis, 2000). The much stronger physical strength of irons allows them to survive in space much longer than stony bodies as seen by their longer cosmic ray exposure ages. Cosmic ray exposure ages record the time an object has spent as a meter-sized

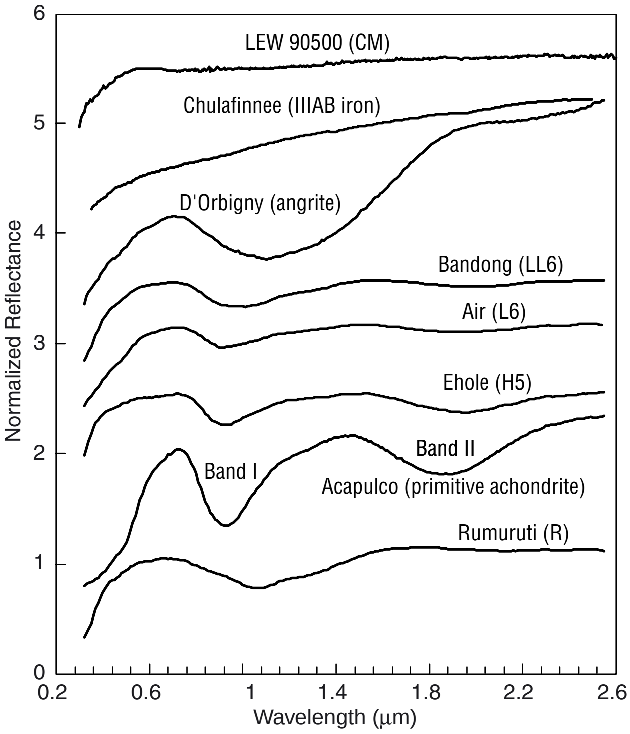

Fig. 1. Reflectance spectra of a number of meteorite types. Spectra are from samples in the Smithsonian's meteorite powder collection except for Chulafinnee (Gaffey 1976) and LEW 90500 (Burbine 1998). All spectra are normalized to unity at 0.55 µm and offset in reflectance from each other. All spectra were taken at RELAB except for the Chulafinnee spectrum.

or less body in space or within a few meters of the surface. Irons have cosmic ray exposure ages ranging from hundreds of millions to a few billion years (e.g. Voshage and Feldman 1979) while stony meteorites tend to have much shorter exposure ages (<100 Ma) (e.g. Marti and Graf 1992, Scherer and Schultz 2000).

Fall statistics

Chondrites, particularly ordinary chondrites (~ 80% of all falls), dominate the flux of meteorites currently landing on Earth (Table 1). Iron meteorites account for only ~ 4% of all falls. We do not understand all the biases that may be present in our fall statistics. For example, many types of carbonaceous chondritic material may be too weak (e.g. Sears 1998) to be able to make it through the atmosphere to Earth's surface as meteorites and may only be sampled as interplanetary dust particles.

Mineral and meteorite spectroscopy

Compositional data on asteroids are usually derived from the analysis of sunlight reflected from their surfaces. A number of minerals (e.g. olivine, pyroxene, hydrated silicates) widely found in meteorites can be identified by their diagnostic spectral properties. Spectral features in the visible and near-infrared (Figure 1) arise from a variety of electronic and vibrational transitions within mineral phases.

Olivine has three absorption bands that make up its feature centered near 1 µm. Pyroxenes tend to have features centered near 0.9–1.0 (Band I) and 1.9–2.0 µm (Band II), although some high-Ca pyroxenes (Adams 1975, Cloutis and Gaffey 1991) do lack a distinctive ~ 2 µm feature (Band II). The ~ 1 and ~ 2 µm features in pyroxenes tend to move to longer wavelengths with increasing Fe and/or Ca-contents. Besides composition, the shapes and depths of absorption bands are functions of other parameters such as particle size (e.g. Johnson and Fanale 1973) and temperature (e.g. Singer and Roush 1985, Hinrichs et al. 1999). These features in olivine and pyroxene are from electronic transitions due to Fe^{2+}.

All of these features can be readily observed in the spectra of various meteorites (Figure 1). The composition of R-chondrite Rumuruti is dominated by olivine, which can be seen in its reflectance spectrum. In contrast, Acapulco's mineralogy is dominated by orthopyroxene, which is reflected in the strong ~ 1 and ~ 2 µm bands that dominate its spectrum. Ordinary chondrites (H, L, and LL chondrites) are mixtures of olivine and pyroxene and have spectral features due to both minerals. The angrite D'Orbigny contains both olivine and a Ti-rich calcic pyroxene (unofficially termed fassaite). Despite containing significant amounts of pyroxene, its spectrum lacks a distinctive ~ 2 µm feature (Burbine et al. 2001c).

One meteoritic material that does not have diagnostic absorption features in the visible and near-infrared is metallic iron (Figure 1). Metallic iron spectra (e.g. Cloutis et al. 1990) tend to be relatively featureless with red spectral slopes and moderate visual albedos (~ 0.10–0.30). (Red refers to the reflectance increasing with increasing wavelength.) Another is the pyroxene enstatite, which has no diagnostic absorption features due to the lack of Fe^{2+}. Pure enstatite is very white with visual albedos greater than ~ 0.5. Mixing metallic iron with silicates tends to weaken the silicate absorption features (e.g. Cloutis et al. 1990).

Water-bearing minerals also have diagnostic spectral features. Bound water and structural OH have a variety of vibrational transitions. A number of these fundamental, combination, and overtone absorptions combine to produce a broad and intense feature in the 3 µm region plus weaker features at 1.4 and 1.9 µm. Absorption features due to water are also present in the atmosphere, which causes problems for any Earth-based telescopic observations. CI, CM, and CR chondrites all have relatively strong 3 µm features (Sato et al. 1997).

Carbonaceous chondrites tend to have much weaker absorption features due to the presence of dark matrix material. For example, CM chondrites (Figure 1) have a number of weak features between 0.6 and 0.9 µm (Vilas and Gaffey 1989). The strongest (~ 5% band strength) of the weak features between 0.6 and 0.9 µm is a band centered at ~ 0.7 µm, attributed to an absorption due to ferric iron (Fe^{3+}) in the phyllosilicates. This 0.7 µm feature in meteorites only seems to be found in the spectra of CM chondrites.

Asteroid observations

This section will detail what we currently think we understand about asteroid compositions. Asteroid spectral surveys (e.g. Zellner et al. 1985, Bus and Binzel 2002a) have primarily been done in the visible due to the peaking of the illuminating solar flux and the relative transparency of the atmosphere at these wavelengths. Near-infrared observations (1-3.5 µm) have now become easier to obtain due to the advent of SpeX (an infrared spectrograph at the Infrared Telescope Facility on Mauna Kea) (e.g. Binzel et al. 2001b).

Asteroids are generally grouped into classes (Table 2) based on their visible spectra (~ 0.4 to ~ 0.9–1.1 µm) and visual albedo (when available). The most widely used taxonomy (Tholen 1984) classifies objects observed in the eight-color asteroid survey (ECAS) (Zellner et al. 1985). Bus and Binzel (2002a) did a CCD spectral survey of over 1300 objects and developed an expanded taxonomy (Bus and Binzel 2002b) with many more classes and subclasses to represent the diversity of spectral properties seen in higher-resolution spectra. Representative spectra of a number of Bus and Binzel (2002a, 2002b) asteroid classes are shown in Figure 2.

As stated earlier, to accurately determine an asteroid's mineralogy, observations are needed in the near-infrared since many minerals have diagnostic features in this wavelength region. Near-infrared asteroid spectra (Gaffey et al. 1993, Rivkin et al. 2000, Burbine and Binzel 2002) at a variety of wavelengths have shown that each class tends to contain a wide variety of mineralogies. Only qualitative mineralogical descriptions will be given for asteroid classes discussed in this paper; quantitative analyses of asteroid compositions (determining the proportion and composition of different mineral species) are very difficult (e.g. Clark, 1995) since an asteroid's reflectance spectrum is a function of a number of factors such as mineralogy, mineral chemistry, particle size, and temperature.

Asteroid taxonomy is based on astronomically observed parameters without regard to composition. However, many asteroid classes have been given letter designations that "imply" specific compositions. This includes the letter "M" for metallic, "S" for siliceous (or stony or stony-iron), and "C" for carbonaceous. (Bus and Binzel (2002b) do not differentiate between E, M, and P asteroids and call them all X objects since there spectra are similar and albedo is not used in their taxonomy.) Since each asteroid class only groups asteroids with specific spectral characteristics, not all objects in a class have to have similar surface mineralogies. For example, it is unknown how many M-class asteroids actually have surfaces similar to iron meteorites. For example, enstatite chondrites (primarily mixtures of metallic iron and enstatite) also have relatively featureless spectra (Gaffey 1976) and similar albedos to metallic iron. Also, a subgroup of M-class asteroids (called the W class) have distinctive 3 µm features (e.g. Rivkin et al. 2000), which apparently indicate hydrated minerals and surface compositions inconsistent with metallic iron.

Radar observations have been used to estimate the metal contents of asteroids (Ostro et al., 2002). Radar experiments of asteroids usually measure the distribution of echo power reflected from an object in time delay and Doppler

Table 2. Asteroid Classes

Class	characteristics
A	Distinctive olivine absorption features
B	Weak UV feature, blue past 0.4 µm, subclass of C types; low albedo (generally less than 0.1)
C[a]	Weak UV feature, flat to reddish past 0.4 µm; low albedo (generally less than 0.10)
D	Very red spectrum; low albedo (usually around 0.05 or less)
E	Flat to slightly red, featureless spectrum; high albedo (> 0.30); usually associated with aubrites
F	Very weak UV feature, flat to bluish past 0.4 µm, subclass of C types; low albedo (< 0.10)
G	Strong UV feature, flat past 0.4 µm, subclass of C class; usually have strong 3 µm features; low albedo (< 0.10)
J	Stronger 1 µm feature than V types; appear to have compositions similar to the HEDs
K	Spectrum intermediate between S and C asteroids; usually associated with CO3/CV3 chondrites
L[b]	Very strong UV feature and then becoming approximately flat
M	Flat to slightly red, featureless spectrum; moderate albedo (0.10-0.30)
O	Weak UV feature out to 0.44 µm, very strong 1 µm feature; type spectrum is 3628 Božněmcová
P	Flat to slightly red, featureless spectrum; low albedo (usually around 0.05 or less)
Q	Strong UV and 1 µm feature; spectrum similar to ordinary chondrites
R	Strong UV and 1 µm feature; type spectrum is 349 Dembowska
S[c]	Strong UV feature; usually has 1 µm feature, indicating olivine and/or pyroxene; moderate albedo (0.10–0.30)
T	Weak UV feature, reddish past 0.4 µm; low albedo (< 0.10)
V	Distinctive 1 and 2 µm features due to pyroxene; appear to have compositions similar to the HEDs
W	M-class visible spectrum with a 3 µm absorption feature
X[d]	Spectrum similar to E, M, or P types, but no albedo information

This table is revised from tables in Wetherill and Chapman (1988), Pieters and McFadden (1994), and Bus and Binzel (2002b). The term "red" refers to reflectances increasing with increasing wavelength and the term "blue" refers to reflectances decreasing with increasing wavelength.

[a] Bus and Binzel (2001b) subdivided the C-class objects into the C, Cb, Cg, Ch, and Cgh subclasses based on CCD spectra. Bus and Binzel (2001b) do not define the F and G classes.

[b] Bus and Binzel (2001b) subdivided the L-class objects into the L and Ld classes based on CCD spectra.

[c] Gaffey et al. (1993) subdivided the S-class objects into the S(I) to S(VII) subclasses on the basis of both visible and near-infrared spectra. Bus and Binzel (2002b) have subdivided the S class into the S, Sa, Sk, Sl, Sq, and Sr subclasses based on CCD spectra.

[d] Bus and Binzel (2002b) subdivided the X-class class objects into the X, Xc, Xe, and Xk subclasses based on CCD spectra.

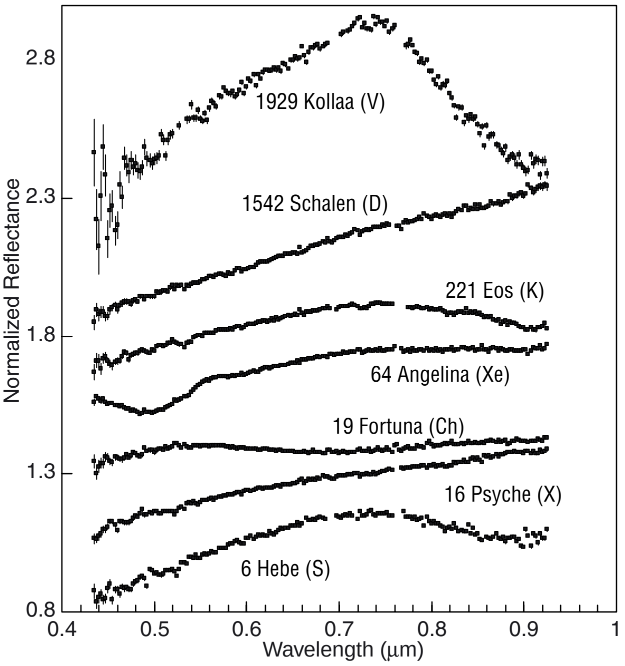

Fig. 2. Reflectance spectra of a number of Bus and Binzel (2002a, 2002b) asteroid classes. All spectra are normalized to unity at 0.55 μm and offset in reflectance from each other. Error bars are one sigma. All spectra are available at the website http://smass.mit.edu.

frequency in the opposite sense (OC) of circular polarization and the same sense. OC radar albedos are equal to the OC radar cross section divided by the target's projected area. For homogeneous and particulate surfaces, radar albedos are functions of the near-surface bulk density, which is related to both the solid-rock density and the surface porosity of the object. Increasing the solid-rock density or decreasing the surface porosity would increase the radar albedo of an object. Without knowing the porosity of the surface, it is impossible to conclusively determine the surface assemblage of an object. M-asteroids with the highest radar albedos (0.6–0.7) could have surfaces of metallic iron with "lunar-like" porosities (35-55%) or solid enstatite-chondritic material with little to no porosity. It is unclear if such solid surfaces of enstatite chondrite material could exist on the surface of an asteroid. M asteroids tend to have higher radar albedos than C or S asteroids (Magri et al. 1999), apparently implying that they are richer in metallic iron.

S asteroids tend to have 1 μm absorption features, which indicates assemblages containing Fe^{2+}-bearing silicates such as olivine and/or pyroxene. On the basis of high-resolution CCD spectra, Bus and Binzel (2002b) subdivide the S asteroids into a number of subtypes (S, Sa, Sk, Sl, Sq, and Sr). The subscript represents that the objects is intermediate in spectral properties between that class (A, K, L, Q, and R) and the S class; however, it is currently unclear if each of these subclasses is grouping objects with similar compositions. From near-infrared spectra, Gaffey et al. (1993) finds that S asteroids tended to have compositions that ranged from olivine-rich (which he defined as S(I)) to pyroxene-rich (S(VII)). To classify these objects, they use the band area ratio (ratio of the area of Band I to the area of Band II) and the Band I minimum, which are both function of the olivine/pyroxene abundance (Cloutis et al., 1986). The band parameters of S(IV)-objects appear consistent with ordinary chondrites, but also consistent with other types of meteorites such as ureilites or acapulcoites/lodranites.

S asteroids are the most abundant type of classified asteroid since they tend to be found in the inner main belt (closer to the Sun) and have higher albedos than C-types, making them brighter and easier to discover and observe. The biggest question concerning S asteroids is what fraction is compositionally similar to ordinary chondrites. S asteroids are spectrally redder than ordinary chondrites and tend to have weaker absorption bands (Figure 3). It has long been argued (e.g. Wetherill and Chapman 1988) whether these spectral differences are due to inherent compositional differences or simply due to an alteration process that can redden ordinary chondrite material. Analyses of lunar regolith (e.g. Pieters et al. 2000) and alteration experiments (e.g. Sasaki et al. 2001) appear to show that this reddening on asteroidal surfaces could be due to surface alteration processes (e.g. micrometeorite impacts, solar wind sputtering) that produce vapor-deposited coatings of nanophase iron.

C-type asteroids (including the B, C, F, G, and P classes) tend to have relatively featureless spectra in low-resolution (photometric) surveys, which was consistent with carbonaceous meteorites. Higher-resolution spectral surveys (e.g. Bus and Binzel 2002b) have shown that almost half of observed C-type asteroids have a 0.7 μm feature. Observations (Jones et al. 1990) indicate that approximately two-thirds of all observed C-type asteroids have 3 μm features.

A-class asteroids tend to have strong UV and 1 μm features that appear similar to those of olivine. Near-infrared spectra (Figure 3) of these objects (Bell et al. 1988) confirm that these surfaces contain significant amounts of olivine as seen by the three distinctive olivine bands that make up the 1 μm feature. Two types of meteorites (brachinites and pallasites) have silicate mineralogies dominated by olivine and have been postulated to have compositions similar to the A asteroids.

V- and J-type asteroids are the asteroids whose mineralogies appear to be the best-determined by remote sensing. These objects (including the 500-km diameter 4 Vesta and much smaller objects with diameters of 10 km or less) have visible and near-infrared spectra (Figure 3) (e.g. McCord et al. 1970, Binzel and Xu 1993, Burbine et al. 2001b) similar to the HEDs, which have very distinctive spectral features due to pyroxene. The smaller V- and J-objects (called Vestoids) have been found in the Vesta family and between Vesta and the 3:1 and the ν_6 resonances. The presence of only one "large" body (4 Vesta) in the main belt with a spectrum similar to HEDs argues that Vesta is the parent body of the HEDs (e.g. Consolmagno and Drake, 1977).

E asteroids, due to their relatively featureless spectra and high albedos (greater than 0.3), have been interpreted as having surfaces composed predominately of an essentially iron-free silicate (e.g. Zellner et al. 1977). The most obvious meteoritic analog is the aubrites (enstatite achondrites), which are igneous meteorites composed primarily of essentially iron-free enstatite (Watters and Prinz 1979). However, the identification of an absorption feature in the 3 µm wavelength region of a number of main-belt E-asteroid spectra (Rivkin et al., 1995) has been interpreted as indicating hydrated minerals on the surfaces of some of these objects, which is inconsistent with an igneous origin. A feature centered at ~ 0.5 µm has also been identified in a number of E-class asteroids (Bus 1999, Fornasier and Lazzarin 2001) and these objects have been classified as Xe by Bus and Binzel (2002b) (Figure 2). This feature is believed to be due to a sulfide (Burbine et al. 2002a), which is commonly found in aubrites (Watters and Prinz 1979).

The surface mineralogies of many other asteroid classes are thought to be somewhat understood. The K-class asteroids tend to have visible and near-infrared spectral properties similar to CO3/CV3 chondrites (Bell 1988, Burbine et al. 2001a, Burbine and Binzel 2002). Q asteroids (most notably 1862 Apollo) tend to have spectral properties similar to ordinary chondrites. D and P objects, which tend to be found in the outer main belt, are thought to have very primitive, organic-rich surfaces due to their relatively featureless and red spectra (e.g. Vilas and Gaffey, 1989). R asteroids (most notably 349 Dembowska) appear to be mixtures of olivine and pyroxene (Gaffey et al., 1989). T asteroids tend to be very dark and featureless and Hiroi and Hasegawa (2002) have noted the spectral similarity of unusual carbonaceous chondrite Tagish Lake to T asteroids.

The surface compositions of a few asteroid classes are unclear, but do appear to contain silicates. O-asteroid 3628 Božněmcová has a 1 µm feature unlike any known meteorite (Burbine and Binzel 2002). L class objects have been newly defined by Bus and Binzel (2002b) and appear intermediate in spectral properties in the visible between the K and some S asteroids.

Spacecraft missions

The first dedicated asteroidal mission was the NEAR-Shoemaker spacecraft rendezvous with S-asteroid 433 Eros (e.g. McCoy et al. 2002) and its flyby of C-asteroid 253 Mathilde (e.g. Veverka et al. 1999). NEAR-Shoemaker Spacecraft obtained high-resolution images, reflectance spectra of different lithologic units, bulk density, magnetic field measurements, and bulk elemental compositions of 433 Eros. Eros had a density of ~ 2.7 g/cm^3, consistent with a silicate-rich assemblage while Mathilde had an extremely low density of 1.3 g/cm^3.

Eros was classified as an S(IV) object (Murchie and Pieters 1996) and it was hoped that the NEAR-Shoemaker data would help "solve" the S-asteroid/ordinary chondrite question. The average olivine to pyroxene composition derived from band area ratios (McFadden et al. 2001) and elemental ratios (Mg/Si, Fe/Si, Al/Si, and Ca/Si) derived from X-ray data (Nittler et al. 2001) of Eros are consistent (McCoy et al. 2001) with ordinary chondrite compositions. However, the S/Si ratio derived from X-ray data (Nittler et al. 2001) and the Fe/O and Fe/Si ratios derived from gamma-ray data (Evans et al. 2001) are significantly depleted relative to ordinary chondrites. McCoy et al. (2001) believe that the best meteoritic analogs to Eros are an ordinary chondrite, whose surface mineralogy has been altered by the depletion of metallic iron and sulfides, or a primitive achondrite, derived from a precursor assemblage of the same mineralogy as one of the ordinary chondrite groups.

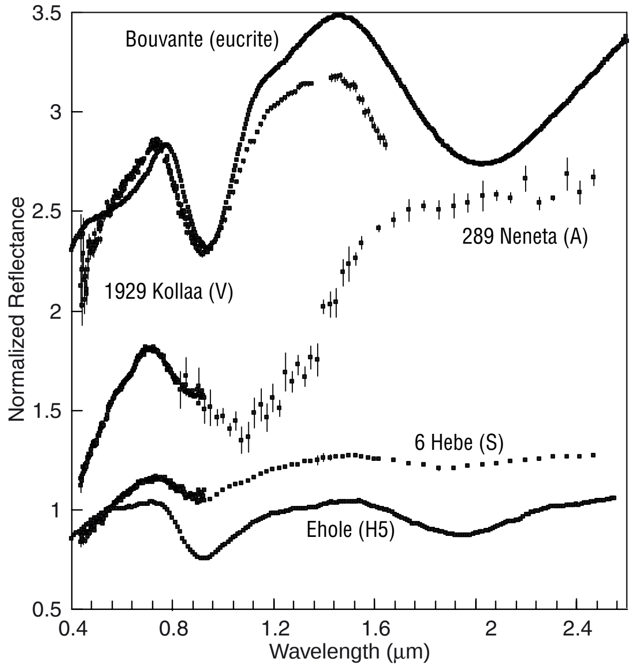

Fig. 3. Reflectance spectra of S-asteroid 6 Hebe versus H5 chondrite Ehole, A-asteroid 289 Nenetta, and 1929 Kollaa versus eucrite Bouvante. The 6 Hebe and 289 Nenetaa spectra are a combination of data from Binzel and Bus (2002a) and Bell et al. (1988) while the 1929 Kollaa spectrum is a combination of data from Binzel and Bus (2002a) and Burbine and Binzel (2002). All spectra are normalized to unity at 0.55 µm and offset in reflectance from each other. Error bars are one sigma. All the Binzel and Bus (2002a) and the Burbine and Binzel (2002) spectra are available at the website http://smass.mit.edu. The Bouvante spectrum is from Burbine et al. (2001b) and was taken at Brown University's RELAB facility.

What is the percentage of near-Earth asteroids with iron meteorite compositions?

What is extremely difficult from Earth to determine is if an object has a composition similar to iron meteorites. This is a problem since for a particular size, the biggest devastation among asteroid impacts will occur for these objects. Metallic iron has no distinctive absorption features and radar observations are often inconclusive since we do not know the surface porosity. There is some evidence that these objects do exist in the near-Earth asteroid population. M-type near-Earth asteroid (6178 1986 DA) (Tedesco and Gradie 1987), has one of the highest radar albedos (~ 0.6) of any observed asteroid, strongly implying a metallic iron surface (Ostro et al. 1991).

Fall percentages give a probability of 4% of an iron meteorite being seen to land on the Earth and a 94% probability of seeing a stony or stony-iron meteorite fall. It is unclear if these fall statistics can be extrapolated to hundreds of meters to tens of kilometer-sized bodies in the near-earth population; however, compositions interpreted from the classifications derived from NEA spectral surveys roughly correspond to these percentages. Binzel et al. (2001a) have published the spectra and classifications of 48 near-Earth asteroids. Approximately 90% of the objects (S, B, C, L, Q, V, O, K) had compositions consistent with silicate-dominated mineralogies if our compositional interpretations of these asteroid classes are correct. Approximately 10% of the objects were classified as X types. As stated before, only some percentage of the X types are probably similar in composition to iron meteorites.

This estimated percentage of iron projectiles is roughly consistent with numbers derived from impact craters. Koerbel (1998) lists 41 impact craters with diameters greater than 100 meters where the compositional characteristics of the impactor have been tentatively identified. He listed 14 (34%) as being due to iron meteorite projectiles with 3 impacts (7%) being due to either chondritic or iron-meteorite assemblages. The rest of the impacts appeared to be due either to chondritic, achondritic, stone, or stony-iron objects. However, the impacts due to iron meteorite assemblages are predominately associated with the smallest craters. Ten of the eleven craters smaller than 1.2 kilometers in diameter are all thought to be due to iron meteorite projectiles. This preponderance of iron meteorite impacts among small craters is due to the atmospheric selection effect (e.g. Melosh 1989) that allows smaller iron meteorite projectiles (since they are denser compared to chondritic ones) to reach the ground and produce hypervelocity impacts. For the 30 craters larger than 2 km in diameter, ~ 25% could be due to iron (or stony-iron) projectiles. However, only one of the eleven craters greater than 24 kilometers in diameter listed by Koeberl (1998) is believed to be due to an asteroid with a composition similar to iron meteorites.

The meteorite fall statistics, classification of NEAs, and the characterization of the impactors that produced large craters all tend to argue that iron meteorite projectiles are a small percentage of the impacting population. All these lines of evidence argue that iron meteorite projectiles are a few percent and certainly less than 10% of near-Earth asteroids. Silicate-dominated assemblages are much more likely to strike the Earth.

Is it important to know the composition of an impacting asteroid?

To estimate the effects of an impact, the mass needs to be known. Since most meteorites that land on the Earth have bulk densities between 2 and 4 g/cm^3, we can estimate pretty well an upper limit on an incoming object's mass by using a density of 4 g/cm^3 and multiplying it by the object's volume computed from its diameter. Also making this mass estimate an upper limit is the fact that asteroids may have significant macroporosity.

But in a real-world situation where a sizable asteroid (e.g. a kilometer in diameter) that will be extremely destructive (~ 5,000 MT) is known to be a collision course with Earth, we will care more about diverting the object than knowing exactly how destructive it will be. Compositional information will be vital for determining how best to divert an object (e.g. Ahrens and Harris 1994). Deflection techniques such as impacting an asteroid with a spacecraft or a nuclear explosion will work best with knowledge of the surface composition. We need to know how the surface will be affected by an impact or blast and this information can only be derived from compositional studies. For example, an asteroid with a composition similar to a carbonaceous chondrite would be expected to fracture much more easily than an object with a composition similar to iron meteorites.

Conclusions

It is certain that the Earth will be hit in the future by an asteroid. The only question is "When?" For this impacting object, compositional studies will be vital for trying to determine how destructive the impact will be and for diverting the object.

Acknowledgments. The author would like to thank Clark Chapman and Guy Consolmagno for very thoughtful reviews and the editorial work of Roman Skála. Almost all of the meteorite spectra in this paper were measured at Brown University's Keck/NASA Reflectance Experiment Laboratory (RELAB), which is a multi-user facility supported by NASA grant NAG5-3871.

References

Adams J. B. (1975): Interpretation of visible and near-infrared diffuse reflectance spectra of pyroxenes and other rock-forming minerals. In: Karr C. III (ed.) Infrared and Raman Spectroscopy of Lunar and Terrestrial Minerals. Academic Press, Inc, New York, pp. 91–116.

Adushkin V. V., Nemchinov I. V. (1994): Consequences of impacts of cosmic bodies on the surface of the Earth. In: Gehrels T. (ed.) Hazards due to Comets and Asteroids. University of Arizona Press, Tucson, pp. 721–778

Ahrens T. J., Harris A. W. (1994): Deflection and fragmentation of near-Earth asteroids. In: Gehrels T. (ed.) Hazards due to Comets and Asteroids. University of Arizona Press, Tucson, pp. 897–927.

Alvarez L., Alvarez W., Asaro F., Michel H. V. (1980): Extraterrestrial cause for the Cretaceous-Tertiary extinction. Science 208, 1095–1108.

Bell J. F. (1988): A probable asteroidal parent body for the CV or CO chondrites (abstract). Meteoritics 23, 256–257.

Bell J. F., Owensby P. D., Hawke B R., Gaffey M. J. (1988): The 52-color asteroid survey: Final results and interpretation (abstract). Lunar Planet. Sci. XIX, 57–58.

Binzel R. P., Xu S. (1993): Chips off of asteroid 4 Vesta: Evidence for the parent body of basaltic achondrite meteorites. Science 260, 186–191.

Binzel, R. P., Harris A. W., Bus S. J., Burbine T. H. (2001a): Spectral properties of near-Earth objects: Palomar and IRTF results for 48 objects including spacecraft targets (9969) Braille and (10302) 1989 ML. Icarus 151, 139–149.

Binzel R. P., Rivkin A. S., Bus S. J., Sunshine J. M., Burbine T. H. (2001b): MUSES-C target asteroid 1998 SF36: A reddened ordinary chondrite. Meteoritics & Planet. Sci. 36, 1167–1172.

Brearley A. J., Jones R. H. (1998): Chondritic meteorites. In: Papike J. J. (ed.) Reviews in Mineralogy, Mineralogical Society of America, Washington, pp. 3-1 to 3-398.

Britt D. T., Consolmagno, G. J. (2001): Modeling the structure of high porosity asteroids. Icarus 152, 134–139.

Britt D. T., Yeoman D., Housen K., Consolmagno G. (2002): Asteroid density, porosity, and structure. In: Bottke W. F. Jr. et al. (eds) Asteroids III. University of Arizona Press, Tucson, pp. 485–500.

Burbine T. H. (1998): Could G-class asteroids be the parent bodies of the CM chondrites? Meteoritics & Planet. Sci. 33, 253–258.

Burbine T. H., Binzel R. P. (2002): Small main-belt asteroid spectroscopic survey in the near-infrared. Icarus 158, 468–499.

Burbine T. H., Binzel R. P., Bus S. J., Clark B. E. (2001a): K asteroids and CO3/CV3 chondrites. Meteoritics & Planet. Sci. 36, 245–253.

Burbine T. H., Buchanan P. C., Binzel R. P., Bus S. J., Hiroi T., Hinrichs J. L., Meibom A., McCoy T. J. (2001b): Vesta, Vestoids, and the HEDs: Relationships and the origin of spectral differences. Meteoritics & Planet. Sci. 36, 761–781.

Burbine T. H., McCoy T. J., Binzel R. P. (2001c): Spectra of angrites and possible parent bodies (abstract). Lunar and Planetary Science XXXIII, Abstract #1857, Lunar and Planet. Inst., Houston, Texas, USA (CD-ROM).

Burbine T. H., Meibom A., Binzel R. P. (1996): Mantle material in the main belt: Battered to bits? Meteoritics & Planet. Sci. 31, 607–620.

Burbine T. H., McCoy T. J., Nittler L. R., Benedix G. K., Cloutis E. A., Dickinson T. L. (2002a): Spectra of extremely reduced assemblages: Implications for Mercury. Meteoritics & Planet. Sci. 37, 1233–1244.

Burbine T. H., McCoy T. J., Meibom A., Gladman B., Keil K. (2002b): Meteoritic parent bodies: Their number and identification. In: Bottke W. F. Jr. et al. (eds) Asteroids III. University of Arizona Press, Tucson, pp. 653–667.

Bus S. J. (1999): Compositional structure in the asteroid belt: Results of a spectroscopic survey. Ph.D. Thesis, Massachusetts Institute of Technology, Cambridge.

Bus S. J., Binzel R. P. (2002a): Phase I of the Small Main-belt Asteroid Spectroscopic Survey: The observations. Icarus 158, 106–145.

Bus S. J., Binzel R. P. (2002b): Phase II of the Small Main-Belt Asteroid Spectroscopic Survey: A feature-based taxonomy. Icarus 158, 146–177.

Chapman C. R., Morrison D. (1994): Impacts on the Earth by asteroids and comets: Assessing the hazard. Nature 367, 33–40.

Chyba C. F., Thomas P. J., Zahnle K. J. (1993): The 1908 Tunguska explosion: Atmospheric disruption of a stony asteroid. Nature 361, 40–44.

Clark B. E. (1995): Spectral mixing models of S-type asteroids. J. Geophys. Res. 100, 14443–14456.

Cloutis E. A., Gaffey M. J. (1991): Pyroxene spectroscopy revisited: Spectral-compositional correlations and relationship to geothermometry. J. Geophys. Res. 96, 22809–22826.

Cloutis, E. A., Gaffey M. J., Jackowski, T. L., Reed K. L. (1986): Calibrations of phase abundance, composition, and particle size distribution for olivine-orthopyroxene mixtures from reflectance spectra. J. Geophys. Res. 91, 11641–11653.

Cloutis E. A., Gaffey M. J., Smith D. G. W., Lambert R. St. J. (1990): Reflectance spectra of “featureless” materials and the surface mineralogies of M- and E-class asteroids. J. Geophys. Res. 95, 281–293.

Consolmagno G. J., Britt D. T. (1998): The density and porosity of meteorites from the Vatican collection. Meteoritics & Planet. Sci.33, 1231–1241.

Consolmagno G. J., Drake M. J. (1977): Composition and evolution of the eucrite parent body: Evidence from rare earth elements. Geochim. Cosmochim. Acta 41, 1271–1282.

Earth Impact Database, 2002. <http://www.unb.ca/passc/ImpactDatabase/> (Accessed: 16 Sept. 2002).

Evans L. G., Starr R. D., Brückner J., Reedy R. C., Boynton W. V., Trombka J. I., Goldsten J. O., Masarik J., Nittler L. R., McCoy T. J. (2001): Elemental composition from gamma-ray spectroscopy of the NEAR-Shoemaker landing site on 433 Eros. Meteoritics & Planet. Sci. 36, 1639–1660.

Flynn G. J., Moore L. B., Klöck W.(1999): Density and porosity of stone meteorites: Implications for the density, porosity, cratering, and collisional disruption of asteroids. Icarus 142, 97–105.

Fornasier S., Lazzarin M. (2001): E-type asteroids: Spectroscopic investigation on the 0.5 µm absorption band. Icarus 152, 127–133.

Gaffey M. J. (1976): Spectral reflectance characteristics of the meteorite classes. J. Geophys. Res. 81, 905–920.

Gaffey M. J., Bell J. F., Cruikshank D. P. (1989): Reflectance spectroscopy and asteroid surface mineralogy. In: Binzel R. P. et al. (eds) Asteroids II. University of Arizona Press, Tucson, pp. 98–127.

Gaffey M. J., Bell J. F., Brown R. H., Burbine T. H., Piatek J. L., Reed K. L., Chaky D. A. (1993): Mineralogical variations within the S-type asteroid class. Icarus 106, 573–602.

Garshnek V., Morrison D., Burkle F. M. Jr. (2000): The mitigation, management, and survivability of asteroid/comet impact with Earth. Space Policy 16, 213–222.

Grady M. M. (2000): Catalogue of Meteorites. Cambridge University Press, Cambridge.

Grossman J. N. (2000): The Meteoritical Bulletin, No. 84, 2000 August. Meteoritics & Planet. Sci. 35, A199–A225.

Grossman J. N., Zipfel J. (2001): The Meteoritical Bulletin, No. 85, 2001 September. Meteoritics & Planet. Sci. 36, A293–A322.

Hildebrand A. R., Pilkington M., Ortiz-Aleman C., Chavez R. E., Urrutia-Fucugauchi J., Connors M., Graniel-Castro E., Camara-Zi A., Halpenny J. F., Niehaus D. (1998): Mapping Chicxulub crater structure with gravity and seismic reflection data. In: Grady M. M. et al. (eds): Meteorites: Flux with Time and Impact Effects. Geological Society, London, pp. 155–176.

Hinrichs J. L., Lucey P. G., Robinson M. S., Meibom A., Krot A. N. (1999): Implications of temperature-dependent near-IR spectral properties of common minerals and meteorites for remote sensing of asteroids. Geophys. Res. Lett. 26, 1661–1664.

Hiroi T., Hasegawa S. (2002): Revisiting the search for the parent body of the Tagish Lake meteorite – Case of a T/D asteroid 308 Polyxo (abstract). Antarctic Meteorites XXVII, 32–33.

Hughes D. W. (1998): The mass distribution of crater-producing bodies. In: Grady M. M. et al. (eds) Meteorites: Flux with Time and Impact Effects. Geological Society, London, pp. 31–42.

Jones T. D., Lebofsky L. A., Lewis J. S., Marley M. S. (1990): The composition and origin of the C, P, and D asteroids: Water as a tracer of thermal evolution in the outer belt. Icarus 88,172–192.

Koeberl C. (1998): Identification of meteoritic components in impactites. In: Grady M. M. et al. (eds) Meteorites: Flux with Time and Impact Effects. Geological Society, London, pp. 133–153.

Lewis J. S. (2000): Comet and asteroid impact hazards on a populated Earth: Computer modeling. Academic Press, San Diego.

Magri C., Ostro S. J., Rosema K. D., Thomas M. L., Mitchell D. L., Campbell D. B., Chandler J. F., Shapiro I. I., Giorgini J. D., Yeomans D. K. (1999): Mainbelt asteroids: Results of Arecibo and Goldstone radar observations of 37 objects during 1980–1985. Icarus 140, 379–407.

Margot J. L., Nolan M. C., Benner L. A. M., Ostro S. J., Jurgens R. F., Giorgini J. D., Slade M. A., Campbell D. B. (2002): Binary asteroids in the near-Earth population. Science 296, 1445–1448.

Marsden B. G., Steel D. I. (1994): Warning times and impact probabilities for long-period comets. In: Gehrels T. (ed.) Hazards due to Comets and Asteroids. University of Arizona Press, Tucson, pp. 221–239.

Marti K., Graf T. (1992): Cosmic-ray exposure history of ordinary chondrites. Ann. Rev. Earth Planet. Sci. 20, 221–243.

McCord T. B., Adams J. B., Johnson T. V. (1970): Asteroid Vesta: Spectral reflectivity and compositional implications. Science 168, 1445–1447.

McCoy T. J., Burbine T. H., McFadden L. A., Starr R. D., Gaffey M. J., Nittler L. R., Evans L. G., Izenberg N., Lucey P. G., Trombka J. I., Bell J. F. III, Clark B. E., Clark P. E., Squyres S. W., Chapman C. R., Boynton W. V., Veverka J. (2001): The composition of 433 Eros: A mineralogical-chemical synthesis. Meteoritics & Planet. Sci. 36, 1661–1672.

McCoy T. J., Robinson M. S., Nittler L. R., Burbine T. H. (2002): The Near Earth Asteroid Rendezvous mission to asteroid 433 Eros: A milestone in the study of asteroids and their relationship to meteorites. Chemie der Erde 62, 89–121.

McFadden L. A., Wellnitz D. D., Schnaubelt M., Gaffey M. J., Bell J. F. III, Izenberg N., Chapman C. R., Murchie S. (2001): Mineralogical interpretation of reflectance spectra of Eros from NEAR near-infrared spectrometer low phase flyby. Meteoritics & Planet. Sci. 36, 1711–1726.

Meibom A., Clark B. E. (1999): Evidence for the insignificance of ordinary chondritic material in the asteroid belt. Meteoritics & Planet. Sci. 34, 7–24.

Melosh H. J. (1989): Impact Cratering: A Geologic Process. Oxford University Press, New York.

Melosh H. J., Tonks W. B. (1993): Swapping rocks: Ejection and exchange of surface material among the terrestrial planets (abstract). Meteoritics & Planet. Sci. 28, 398.

Milner A. C. (1998): Timing and causes of vertebrate extinction across the Cretaceous-Tertiary boundary. In: Grady M. M. et al. (eds) Meteorites: Flux with Time and Impact Effects. Geological Society, London, pp. 247–257.

Mittlefehldt D. W. (2002): Geochemistry of the ungrouped carbonaceous chondrite Tagish Lake, the anomalous CM chondrite Bells, and comparison with CI and CM chondrites. Meteoritics & Planet. Sci. 37, 703–712.

Mittlefehldt D. W., McCoy T. J., Goodrich C. A., Kracher A. (1998): Non-chondritic meteorites from asteroidal bodies. In: Papike J. J. (ed.) Reviews in Mineralogy, Mineralogical Society of America, Washington, pp. 4-1 to 4-195.

Morbidelli A., Jedicke R., Bottke W. F., Michel P., Tedesco E. F. (2002): From magnitudes to diameters: The albedo distribution of near Earth objects and the Earth collision hazard. Icarus 158, 329–342.

Morgan J., Warner M., Grieve R. (2002): Geophysical constraints on the size and structure of the Chicxulub impact crater. In: Grady M. M. et al. (eds.) Meteorites: Flux with Time and Impact Effects. Geological Society, London, pp. 39–46.

Murchie S. L., Pieters C. M. (1996): Spectral properties and rotational spectral heterogeneity of 433 Eros. J. Geophys. Res. 101, 2201–2214.

Neukum G., Ivanov B. A. (1994): Crater size distributions and impact probabilities on Earth from lunar, terrestrial-planet, and asteroid cratering data. In: Gehrels T. (ed.) Hazards due to Comets and Asteroids. University of Arizona Press, Tucson, pp. 359–416.

Nittler L. R., Starr R. D., Lim L., McCoy T. J., Burbine T. H., Reedy R. C., Trombka J. I., Gorenstein P., Squyres S. W., Boynton W. V., McClanahan T. P., Bhangoo J. S., Clark P. E., Murphy M. E., Killen R. (2001): X-ray fluorescence measurements of the surface elemental composition of asteroid 433 Eros. Meteoritics & Planet. Sci. 36, 1673–1695.

Ostro S. J., Campbell D. B., Chandler J. F., Hine A. A., Hudson R . S., Rosema K. D., Shapiro I. I. (1991): Asteroid 1986 DA: Radar evidence for a metallic composition. Science 252, 1399–1404.

Ostro S. J., Hudson R. S., Benner L. A. M., Giorgini J. D., Magri C., Margot J. L., Nolan M. (2002): Asteroid radar astronomy. In: Bottke W. F. Jr. et al. (eds) Asteroids III. University of Arizona Press, Tucson, pp. 151–168.

Paine M. P. (1999): Asteroid impacts: The extra hazard due to tsunami. Science of Tsunami Hazards 17, 155–172.

Pieters C. M., McFadden L. A. (1994): Meteorite and asteroid reflectance spectroscopy: Clues to the early solar system processes. Ann. Rev. Earth Planet. Sci. 22, 457–497.

Pieters C. M., Taylor L. A., Noble S. K., Keller L. P., Hapke B., Morris R. V., Allen C. C., McKay D. S., Wentworth S. (2000): Space weathering on airless bodies: Resolving a mystery with lunar samples. Meteoritics & Planet. Sci. 35, 1101–1107.

Rivkin A. S., Lebofsky L. A., Clark B. E., Howell E. S., Britt D. T. (2000): The nature of M-class asteroids from 3-μm observations. Icarus 145, 351–368.

Sasaki S., Nakamura K. Hamabe Y., Kurahashi E., Hiroi T. (2001): Production of iron nanoparticles by laser irradiation in a simulation of lunar-like space weathering. Nature 410, 555–557.

Sato K., Miyamoto M., Zolensky M. E. (1997): Absorption bands near three micrometers in diffuse reflectance spectra of carbonaceous chondrites: Comparison with asteroids. Meteoritics & Planet. Sci. 32, 503–507.

Scherer P., Schultz L. (2000): Noble gas record, collisional history, and pairing of CV, CO, CK, and other carbonaceous chondrites. Meteoritics & Planet. Sci. 35, 145–153.

Scott E. R. D. (2001): Formation of mesosiderites by fragmentation and reaccretion of a large differentiated asteroid. Meteoritics & Planet. Sci. 36, 869–881.

Sears D. W. G. (1998): The case for rarity of chondrules and CAI in the early solar system and some implications for astrophysical models. Astrophys. J. 498, 773–778.

Singer R. B., Roush T. L. (1985): Effects of temperature on remotely sensed mineral absorption features. J. Geophys. Res. 90, 12434–12444.

Stuart J. S. (2001): Near-Earth asteroid population from the LINEAR survey. Science 294, 1691–1693.

Tedesco E. F., Gradie J. (1987): Discovery of M class objects among the near-Earth asteroid population. Astron. J. 93, 738–746.

Tholen D. J. (1984): Asteroid taxonomy from cluster analysis of photometry. Ph.D. Thesis, Univ. Arizona, Tucson.

Toon O. B., Zahnle K., Morrison D., Turco R. P., Covey C. (1997): Environmental perturbations caused by the impacts of asteroids and comets. Rev. Geophysics 35, 41–78.

Vasilyev N. V. (1998): The Tunguska Meteorite problem today. Planetary & Space Sciences 46, 129–150.

Veverka J, Thomas P., Harch A., Clark B., Bell J. F. III., Carcich B., Joseph, J., Murchie S., Izenberg N., Chapman C., Merline W., Malin M., McFadden L., Robinson M. (1999): NEAR encounter with asteroid 253 Mathilde: Overview. Icarus 140, 3–16.

Vilas F., Gaffey M. J. (1989): Phyllosilicate absorption features in main-belt and outer-belt asteroid reflectance spectra. Science 246, 790–792.

Voshage H., Feldman H. (1979): Investigations on cosmic-ray produced nuclides in iron meteorites, 3. Exposure ages, meteoroid sizes and sample depths determined by mass spectrometric analyses of potassium and rare gases. Earth Planet. Sci. Lett. 45, 293–308.

Wasson J. T. (1995): Sampling the asteroid belt: How biases make it difficult to establish meteorite-asteroid connections (abstract). Meteoritics 30, 595.

Watters T. R., Prinz M. (1979): Aubrites: Their origin and relationship to enstatite chondrites. Proc. Lunar Planet. Sci. Conf. 10th, 1073–1093.

Weisberg M. K., Prinz M., Clayton R. N., Mayeda T. K., Sugiura N., Zashu S., Ebihara M. (2001): A new metal-rich chondrite grouplet. Meteoritics & Planet. Sci. 36, 401–418.

Wetherill G. W., Chapman C. R. (1988): Asteroids and meteorites. In: Kerridge J. F., Matthews M. S. (eds) Meteorites and the Early Solar System. University of Arizona Press, Tucson, pp. 35–67.

Wilkison S. L., Robinson M. S. (2000): Bulk density of ordinary chondrite meteorites and implications for asteroidal internal structure. Meteoritics & Planet. Sci. 35, 1203–1213.

Yeomans D. K., Antreasian P. G., Barriot J. -P., Chesley S. R., Dunham D. W., Farquhar R. W., Giorgini J. D., Helfrich C. E., Konopliv A. S., McAdams J. V., Miller J. K., Owen W. M Jr., Scheeres D. J., Thomas P. C., Veverka J., Williams B. G. (2000): Radio science results during the NEAR-Shoemaker rendezvous with Eros. Science 289, 2085–2088.

Zellner B., Leake M., Morrison D., Williams J. G. (1977): The E asteroids and the origin of the enstatite achondrites. Geochim. Cosmochim. Acta 41, 1759–1767.

Zellner B., Tholen D. J., Tedesco E. F. (1985): The eight-color asteroid survey: Results for 589 minor planets. Icarus 61, 355–416.

Handling editor: Roman Skála